Cellular/Molecular

Motoneurons Express Heteromeric TWIK-Related Acid-Sensitive K^+ (TASK) Channels Containing TASK-1 (KCNK3) and TASK-3 (KCNK9) Subunits

Allison P. Berg,[1] Edmund M. Talley,[1] Jules P. Manger,[1] and Douglas A. Bayliss[1,2]
Departments of [1]Pharmacology and [2]Anesthesiology, University of Virginia, Charlottesville, Virginia 22908

Background potassium currents carried by the KCNK family of two-pore-domain K^+ channels are important determinants of resting membrane potential and cellular excitability. TWIK-related acid-sensitive K^+ 1 (TASK-1, KCNK3) and TASK-3 (KCNK9) are pH-sensitive subunits of the KCNK family that are closely related and coexpressed in many brain regions. There is accumulating evidence that these two subunits can form heterodimeric channels, but this evidence remains controversial. In addition, a substantial contribution of heterodimeric TASK channels to native currents has not been unequivocally established. In a heterologous expression system, we verified formation of heterodimeric TASK channels and characterized their properties; TASK-1 and TASK-3 were coimmunoprecipitated from membranes of mammalian cells transfected with the channel subunits, and a dominant negative TASK-1(Y191F) construct strongly diminished TASK-3 currents. Tandem-linked heterodimeric TASK channel constructs displayed a pH sensitivity (pK ~7.3) in the physiological range closer to that of TASK-1 (pK ~7.5) than TASK-3 (pK ~6.8). On the other hand, heteromeric TASK channels were like TASK-3 insofar as they were activated by high concentrations of isoflurane (0.8 mM), whereas TASK-1 channels were inhibited. The pH and isoflurane sensitivities of native TASK-like currents in hypoglossal motoneurons, which strongly express TASK-1 and TASK-3 mRNA, were best represented by TASK heterodimeric channels. Moreover, after blocking homomeric TASK-3 channels with ruthenium red, we found a major component of motoneuronal isoflurane-sensitive TASK-like current that could be attributed to heteromeric TASK channels. Together, these data indicate that TASK-1 and TASK-3 subunits coassociate in functional channels, and heteromeric TASK channels provide a substantial component of background K^+ current in motoneurons with distinct modulatory properties.

Key words: **potassium channel; TASK; KCNK; heterodimer; isoflurane; ruthenium red; hypoglossal; rat**

Introduction

Potassium "leak" channels, which are active at resting membrane potential and show little voltage dependence, are important determinants of resting membrane potential and cellular excitability. Although neuronal leak K^+ channels escaped detection at the molecular level for many years, it has now become clear that the newly identified KCNK family of potassium channel subunits contribute to these currents in many cell types (Goldstein et al., 2001; Bayliss et al., 2003; Lesage, 2003; Talley et al., 2003). The membrane topology proposed for KCNK channel subunits is unique among cloned K^+ channels insofar as it includes two pore domains in a single subunit, rather than one, predicting that only two KCNK subunits are needed to assemble a pseudotetrameric K^+-selective pore.

The TWIK-related acid-sensitive K^+ (TASK) channels are a subgroup of the KNCK channel family, with TASK-1 (KCNK3) and TASK-3 (KCNK9) representing the functional members of that group (Lesage and Lazdunski, 2000; Patel and Honore, 2001; Rajan et al., 2001; Bayliss et al., 2003; Talley et al., 2003). These two channel subunits share a number of properties when expressed individually in heterologous expression systems. As their name suggests, they are sensitive to changes in extracellular pH; both are activated by alkalization and inhibited by acidification, although over different pH ranges (pK values for channel activity, ~7.5 and ~6.8 for TASK-1 and TASK-3, respectively) (Duprat et al., 1997; Kim et al., 1998, 2000; Leonoudakis et al., 1998; Chapman et al., 2000; Rajan et al., 2000). In addition, each subunit produces whole-cell currents with voltage-dependent and kinetic properties of instantaneous open rectifiers, and both are activated by inhalation anesthetics and inhibited downstream of G-protein-coupled receptors (Patel et al., 1999; Czirjak et al., 2000; Sirois et al., 2000; Talley et al., 2000; Meadows and Randall, 2001; Talley and Bayliss, 2002; Chemin et al., 2003).

A common but not universal feature among closely related potassium channel subunits is their ability to coassemble, with association of different subunits often leading to heteromeric channels with properties discrete from those of the constituent subunits. This combinatorial potential provides a mechanism for additional diversity in K^+ channel properties within individual

Received April 14, 2004; revised May 30, 2004; accepted June 8, 2004.

This work was supported by a scientist development grant from the American Heart Association (E.M.T.) and by National Institutes of Health Grants NS33583 and GM66181 (D.A.B.). E.M.T. is a Parker B. Francis fellow in pulmonary research. We thank Dr. J. C. Lawrence for help with affinity purification of the TASK-3 antibody and Dr. X. Chen for help with gas chromatography.

Correspondence should be addressed to Douglas A. Bayliss, Department of Pharmacology, Box 448, 5015 Jordan Hall, University of Virginia, Charlottesville, VA 22908. E-mail: dab3y@virginia.edu.

DOI:10.1523/JNEUROSCI.1408-04.2004

 0270-6474/04/246693-10$15.00/0

cells (Wei et al., 1990; Krapivinsky et al., 1995; Wang et al., 1998), but evidence in support of native heterodimeric channels of the KCNK family is scarce (Kang et al., 2003). In the case of TASK-1 and TASK-3, heterodimeric channels have been detected in heterologous expression systems (Czirjak and Enyedi, 2002a; Kang et al., 2003; Lauritzen et al., 2003; but see Karschin et al., 2001; Pei et al., 2003), and a substantial overlap of subunit expression in many areas of the CNS provides a substrate for their coassembly *in vivo* (Karschin et al., 2001; Talley et al., 2001; Vega-Saenz de Miera et al., 2001). In cerebellar granule neurons that express TASK-1 and TASK-3, coassociation of TASK channels into functional native heterodimers was demonstrated by taking advantage of the unique single-channel properties and ruthenium red sensitivity defined for recombinant linked heterodimeric TASK-1/TASK-3 channels (Kang et al., 2003). However, the relative contribution of those heterodimeric TASK channels to granule neuron whole-cell current remains uncertain (Kang et al., 2003; Lauritzen et al., 2003). The existence and relative contribution of heterodimeric TASK channels in other neuronal cell groups that coexpress TASK-1 and TASK-3 subunits has not been determined.

In the CNS, somatic motoneurons display some of the highest levels of TASK-1 and TASK-3 expression (Karschin et al., 2001; Talley et al., 2001). Accordingly, we found open-rectifier currents in those motoneurons that were pH-sensitive, activated by inhalational anesthetics, and inhibited by G-protein-coupled receptors (Sirois et al., 2000; Talley et al., 2000). At that time, which preceded the cloning of TASK-3, we attributed the native motoneuronal current to TASK-1 because the pK for inhibition was ~7.4, essentially identical to that of TASK-1 (Sirois et al., 2000; Talley et al., 2000). However, in light of current evidence for strong expression of TASK-3 in motoneurons (Karschin et al., 2001; Talley et al., 2001; Vega-Saenz de Miera et al., 2001), we suspected that those subunits could contribute to native TASK-like motoneuronal currents, perhaps paired with TASK-1 in heterodimeric channels. In the present study, we used biochemical and electrophysiological approaches in a heterologous expression system to demonstrate formation of heterodimeric TASK channels and to characterize their properties. We further show that, unlike in other cell systems studied to date, the whole-cell TASK-like currents in rat hypoglossal motoneurons include a major contribution from heterodimeric TASK channels.

Materials and Methods

Channel constructs. Constructs were generated as described previously (Talley and Bayliss, 2002). Rat TASK-1 (GenBank accession number AF031384) and TASK-3 (GenBank accession number AF391084) were subcloned into mammalian expression vector pcDNA3 (Invitrogen, Carlsbad, CA). A triple hemagglutinin (HA) epitope tag was added to the N terminus of wild-type channels by excising the relevant sequence from pKH3 (Mattingly et al., 1994) and inserting it in-frame with the TASK channel coding sequence in pcDNA3. N-terminal green fluorescent protein (GFP)-tagged TASK channel constructs were produced by subcloning TASK channel cDNA into pEGFP (Clontech, Palo Alto, CA). Tandem heterodimeric TASK-1/TASK-3 and TASK-3/TASK-1 constructs were generated by PCR to generate a final product bearing a three-residue (glycine-serine-alanine) linker region between the C-terminal amino acid of the first subunit and the start methionine of the second subunit. Constructs containing a Y191F substitution were generated in TASK-1 and TASK-3 by PCR. All constructs were fully verified by sequence analysis.

Tissue culture and transfections. Human embryonic kidney (HEK) 293 cells stably expressing the thyrotropin-releasing hormone receptor [E2 cells (Kim et al., 1994); obtained from Graeme Milligan (University of Glasgow, Scotland, UK)] were maintained in DMEM/F-12 containing 10% FBS, penicillin (100 U/ml), and streptomycin (100 μg/ml) and supplemented with G418 (400 μg/ml; Invitrogen). All constructs were transfected using LipofectAMINE 2000 (Invitrogen) according to the manufacturer's instructions. E2 cells were cotransfected with channel clones and GFP (pGreen Lantern; Invitrogen). Cells were plated onto poly-L-lysine (100 μg/ml)-coated glass coverslips ~12–16 hr after transfection and allowed to adhere for 1 hr at 37°C before recording.

Brainstem slice preparation. All animal use was in accordance with guidelines approved by the University of Virginia Animal Care and Use Committee. Transverse slices were prepared from brainstems of neonatal Sprague Dawley rats (postnatal days 7–14) as described previously (Sirois et al., 1998). Rats were anesthetized with ketamine and xylazine; brainstems were removed after rapid decapitation. Slices (300 μm) were cut with a microslicer (DSK 1500E; Dosaka) in an ice-cold substituted Ringer's solution consisting of (in mM): 260 sucrose, 3 KCl, 5 $MgCl_2$, 1 $CaCl_2$, 1.25 NaH_2PO_4, 26 $NaHCO_3$, 10 glucose, and 1 kynurenic acid. Slices were incubated for 1 hr at 37°C and subsequently at room temperature in a normal Ringer's solution containing (in mM): 130 NaCl, 3 KCl, 2 $MgCl_2$, 2 $CaCl_2$, 1.25 NaH_2PO_4, 26 $NaHCO_3$, and 10 glucose. Both substituted and normal Ringer's solutions were bubbled with 95% O_2 and 5% CO_2.

Electrophysiology. For recording, E2 cells were visualized under infrared differential interference contrast (DIC) and epifluorescent optics, and transfected cells were selected using GFP fluorescence. Slices were visualized with infrared DIC optics, and hypoglossal motoneurons were identified by their anatomic location and their characteristic size and shape. All recordings were performed at room temperature. Recording pipettes were pulled from borosilicate glass capillaries to a DC resistance ranging from 3 to 5 MΩ and coated with Sylgard 184 (Dow Corning, Midland, MA). The pipette solution was (in mM): 120 KCH_3SO_3, 4 NaCl, 1 $MgCl_2$, 0.5 $CaCl_2$, 10 HEPES Na, 10 EGTA, 3 ATP, and 0.3 GTP; the bath solution contained (in mM): 140 NaCl, 3 KCl, 10 HEPES Na, 10 glucose, 2 $CaCl_2$, and 2 $MgCl_2$. For recordings from motoneurons, the pipette solution contained 50 μM ZD7288 (Tocris Cookson, Ellisville, MO) to block pH- and anesthetic-sensitive I_h in motoneurons; we also added 0.5 μM tetrodotoxin (Alomone Labs, Jerusalem, Israel) to the bath solution, and, where noted, we included 10 μM ruthenium red (Sigma, St. Louis, MO). Isoflurane was bubbled into the bath solutions through a calibrated vaporizer. Isoflurane concentrations were determined by gas chromatography from samples collected at the point of solution entry into the recording chamber (Sirois et al., 1998).

Data acquisition and analysis. Voltage commands were applied, and currents were recorded using pCLAMP software interfaced with an Axopatch 200A amplifier via a Digidata 1320A digitizer (all from Axon Instruments, Foster City, CA). Series resistance was compensated by 60–75% and was monitored throughout the recordings to ensure adequate compensation. Cells were held at −60 mV, and depolarizing ramps (0.2 V/sec, from −130 to −20 mV) were applied at 5 sec intervals for transfected HEK 293 cells. For analysis, slope conductance was evaluated by linear fits to currents from −130 to −60 mV. Concentration–response curves of normalized data were fitted by using logistic equations of the form: $G = 1/(1 + (a/b)^c)$, where G represents normalized conductance; a, concentration or pH; b, the EC_{50} or pK; and c, the Hill coefficient. The Hill coefficient obtained in the pH domain (c) is expressed as a function of hydrogen ion concentration (c') by: $c' = -c * 0.434/\text{pK}$. Statistical analyses were performed by Student's t test and ANOVA, with significance accepted at $p < 0.05$.

Crude membrane preparations of E2 cells. E2 cells were transfected in 10 cm^2 tissue culture dishes using LipofectAMINE 2000, and after ~16 hr, the cells were washed with PBS and harvested into 1 ml of Tris-EDTA (TE) containing the protease inhibitors leupeptin (2 μg/ml), PMSF (100 μM), pepstatin (2 μg/ml), and aprotinin (2 μg/ml). Cells were mechanically disrupted with 20–25 strokes in a Dounce homogenizer, and the lysate was centrifuged at 4°C for 5 min at 500 × g. The supernatant was centrifuged at 4°C for 30 min at 60,000 rpm in a Beckman XL-90 apparatus using a Ti90 rotor. The pellet from this high-speed spin was resuspended in TE plus protease inhibitors using a 19 gauge syringe needle.

Immunoprecipitation and Western blots. E2 cell membranes were solubilized for 1 hr at 4°C in lysis buffer (in %: 0.1 SDS, 1 Triton X-100, and

1 sodium deoxycholate in TE). Antibodies for immunoprecipitation were used at 5 μg/ml and incubated for 1 hr at 4°C with solubilized membranes. Protein A-conjugated agarose beads (Invitrogen) were prewashed in lysis buffer containing 10 mg/ml bovine serum albumin (BSA) and incubated with membrane–antibody mixtures for 1 hr at 4°C. Beads were washed in lysis buffer with BSA and then in TE before eluting immunoprecipitated proteins in sample loading buffer (50% glycerol, 5% β-mercaptoethanol, 2.3% SDS and 0.0625 M Tris-H_3PO_4) for 1.5 hr at 37°C. Proteins were separated on 10% SDS-PAGE and electrotransferred to nitrocellulose membranes. Antibodies requiring enhanced chemiluminescence (ECL) detection of horseradish peroxidase (HRP) conjugates were diluted in 5% milk in Tris-buffered saline containing 0.1% Tween 20 (TBST), with avidin–biotin detection performed in 1% BSA in TBST.

Antibodies. Serum from rabbits immunized with the peptide CRVEEIPPDVLRNTY (derived from the C terminus of rat TASK-3) was obtained from Sigma Genosys (The Woodlands, TX) and purified by affinity chromatography. This antibody ($T3_2$) specifically recognized TASK-3 in lysates from E2 cells transfected with TASK channel subunits and revealed a brain distribution consistent with previous *in situ* hybridization results (see Fig. 1*A*). We obtained monoclonal rat anti-HA-HRP (1:10,000) from Roche Molecular Biochemicals (Indianapolis, IN) and mouse anti-transferrin receptor (1:1000) from Zymed (San Francisco, CA). $T3_2$ was biotinylated using an EZ-Link Sulfo-NHS-LC Biotinylation kit according to manufacturer's protocol (Pierce, Rockford, IL). Unconjugated antibodies were detected using HRP-conjugated IgG secondary antibodies from Amersham Biosciences (Piscataway, NJ). Biotinylated antibodies were detected using avidin–biotin complex from Vector Labs (Burlingame, CA). HRP conjugates were visualized using ECL developed on ECL Hyperfilm (Amersham Biosciences). Control blocking experiments (plus peptide) were performed by preincubating TASK channel antibodies with 10× concentrations of corresponding antigenic peptides.

Immunohistochemistry. For immunohistochemistry on tissue sections, Sprague Dawley rats (300 gm) were perfused transcardially with heparin-containing saline and then 4% paraformaldehyde (PFA) in phosphate buffer, pH 7.4. The brains were removed, postfixed overnight in 4% PFA, and then blocked and cut at 30 μm on a vibratome. The sections were washed extensively in a series of phosphate- and Tris-buffered saline (TS) solutions and then preblocked for 1 hr in 3% goat serum and 0.5% Triton X-100 and TS. Sections were incubated at 4°C for 48 hr with affinity-purified rabbit anti-TASK-3 ($T3_2$; at 1:5000–1:10,000) and then successively with a biotinylated goat anti-rabbit secondary antibody and an avidin–biotin–HRP complex for 1 hr each at room temperature (ABC Elite kit; Vector Laboratories). The HRP was detected by using diaminobenzidine (DAB) according to the manufacturer's instructions, with nickel enhancement (DAB substrate kit; Vector Laboratories). Sections were air-dried, dehydrated in ethanol and xylene, and coverslipped (DPX; BDH, Poole, UK). Cells immunoreactive for TASK-3 were visualized on a Zeiss (Thornwood, NY) FS microscope equipped with a QImaging Retiga 1300C digital camera, and images were obtained using IPLab software (Scanalytics). In control experiments, we found no cellular staining when the primary antibody was omitted from the protocol or preincubated with a 10× concentration of antigenic peptide (data not shown).

Results

Biochemical association of TASK-1 and TASK-3 in HEK 293 cells

We produced and characterized an anti-peptide TASK-3 antibody ($T3_2$) to use in coimmunoprecipitation studies in order to determine whether TASK-1 and TASK-3 subunits can associate in a heterologous expression system. As depicted in Figure 1*A* (top), the $T3_2$ antibody specifically and selectively detected the appropriate TASK channel subunit in lysates from transfected cells. It identified a set of bands only in cells transfected with the corresponding TASK-3 channel subunit; the immunoreactivity was blocked by preadsorption with the cognate antigenic peptide and was identical to that detected with monoclonal antibodies against an HA epitope tag incorporated into the TASK-3 subunit. The $T3_2$ antibody did not detect the corresponding HA-TASK-1; expression of this construct was verified using the anti-HA antibody. The same set of immunoreactive bands were obtained in blots from cells transfected with untagged TASK-3 subunits (data not shown), and incorporation of the HA tag had no effect on TASK channel currents recorded from HEK 293 cells (Talley and Bayliss, 2002).

We also characterized this $T3_2$ antibody by immunohisto-

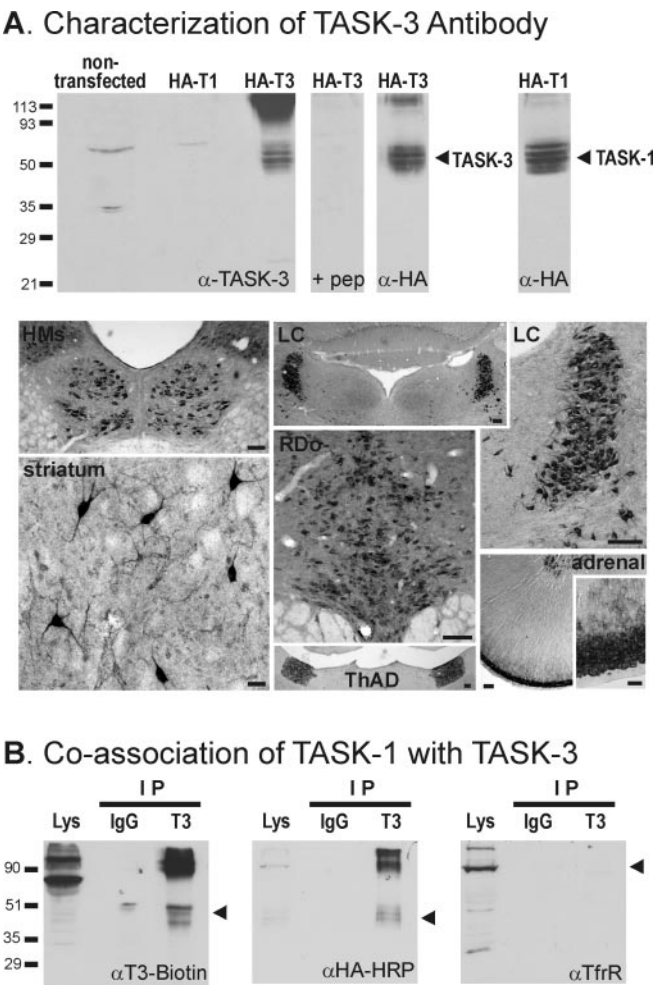

Figure 1. TASK-1 coimmunoprecipitates with TASK-3 in HEK 293 cells. *A*, Characterization of TASK-3 antibody. Top, Lanes were loaded with 5 μg of membrane preparations from HEK 293 cells transfected with the indicated constructs, and proteins were separated by 10% SDS-PAGE. Epitope-tagged HA-TASK-3 (T3) was identified with the anti-TASK-3 antibody; no immunoreactivity was seen for the corresponding HA-TASK-1 (T1) channel construct, or for HA-TASK-3 when the antibody was preadsorbed with excess antigenic peptide (pep). Essentially identical bands were recognized with an antibody to the epitope (α-HA), which was also used to confirm expression of HA-TASK-1. Bottom, Immunohistochemistry was used to detect TASK-3 distribution in sections of rat brain and adrenal gland. TASK-3-like immunoreactivity was detected in a distribution pattern that was strikingly similar to previous TASK-3 *in situ* hybridization reports (Karschin et al., 2001; Talley et al., 2001; Vega-Saenz de Miera et al., 2001; Bayliss et al., 2003). Especially strong labeling was seen in cell bodies from the following regions (clockwise from top left): hypoglossal motor nucleus (HMs), locus ceruleus (LC), adrenal gland, anterodorsal thalamic nucleus (ThAD), dorsal raphe nucleus (RDo), and striatum. Scale bars: striatum, adrenal inset, 50 μm; others, 100 μm. *B*, HEK 293 cells were cotransfected with TASK-3 and HA-TASK-1 constructs. The TASK-3 antibody coimmunoprecipitated (IP) TASK-3 (left) and HA-TASK-1 (middle) but did not immunoprecipitate transferrin receptor (TfrR), an endogenously expressed membrane protein (right); a control nonspecific rabbit IgG did not immunoprecipitate either TASK subunit. Molecular weight markers (kilodaltons) are indicated on the left; arrowheads indicate locations of precipitated proteins.

chemistry; the distribution of TASK-3 expression observed with this antibody was remarkably similar to that obtained by *in situ* hybridization (Karschin et al., 2001; Talley et al., 2001; Vega-Saenz de Miera et al., 2001; Bayliss et al., 2003). As shown in Figure 1*A* (bottom), we found strong immunostaining in all motoneurons, including hypoglossal motoneurons, which are the focus of this study and in which we have previously described robust TASK-like currents (Sirois et al., 2000; Talley et al., 2000). Immunoreactivity was particularly strong in cell bodies of presumptive aminergic neurons, including neurons of the locus ceruleus and dorsal raphe nucleus, both of which express high levels of TASK-3 mRNA and display TASK-like currents in whole-cell recordings (Sirois et al., 2000; Washburn et al., 2002). Forebrain neurons likely to be cholinergic were also strongly labeled by this antibody, including large neurons in the striatum (Fig. 1*A*) and in the basal forebrain (data not shown). One other nucleus of note was the anterodorsal thalamic nucleus, which also contains particularly high levels of TASK-3 mRNA (Karschin et al., 2001; Talley et al., 2001; Vega-Saenz de Miera et al., 2001). Outside the CNS, TASK-3 immunoreactivity was extremely high in the adrenal gland, again as expected given earlier functional and RNA expression studies (Czirjak and Enyedi, 2002b; Bayliss et al., 2003); in the adrenal gland, immunostaining was readily apparent in the medulla and was extremely intense in the outer cortex, particularly in the zona glomerulosa (Bayliss et al., 2003). The striking correspondence between these immunohistochemical results detecting TASK-3 protein and previous data on TASK-3 mRNA distribution provide strong validation of the specificity of the $T3_2$ antibody.

Consistent with coassociation of TASK channel subunits, we found that both TASK-3 (Fig. 1*B*, left) and TASK-1 (Fig. 1*B*, middle) were concentrated in TASK-3 immunoprecipitates when HA-TASK-1 and TASK-3 were coexpressed. This was a specific interaction because neither subunit was precipitated with preimmune rabbit IgG and because the TASK-3 antibody did not precipitate another membrane-associated protein, the transferrin receptor (Fig. 1*B*, right). Moreover, the TASK-3 antibody did not immunoprecipitate TASK-1 from cells in which TASK-3 was not coexpressed (data not shown). These data indicate that TASK-1 and TASK-3 can associate in membranes of HEK 293 cells transfected with both channel subunits.

TASK-1 and TASK-3 associate functionally in HEK 293 cells

The kinetic and voltage-dependent properties of whole-cell currents generated from TASK-1 and TASK-3 homomeric channels are very similar, suggesting that it may be difficult to identify emergent properties that can be attributed to heteromeric channels when the subunits are coexpressed. For this reason, we used a dominant negative approach to demonstrate that the subunit association we detected biochemically indeed reflects a functional association. A number of mutations of the K^+ channel signature sequence analogous to those known to act in a dominant negative manner in the context of other K^+ channels (e.g., GYG → AWA or SYG) (Nakamura et al., 1997; Schroeder et al., 2000), in either or both of the two pore domains, were not useful because they did not block ion conduction but rather rendered the mutated channels nonselective to cations (data not shown). However, we found that a TASK-1 construct containing a Y191F substitution immediately upstream of the signature sequence in the second pore domain was able to act as a dominant negative (Fig. 2); this mutation is analogous to the W → F mutations that abolish ionic currents in *Shaker* and other Kv channels (Perozo et al., 1993; Malin and Nerbonne, 2000). As shown in Figure 2*A*,

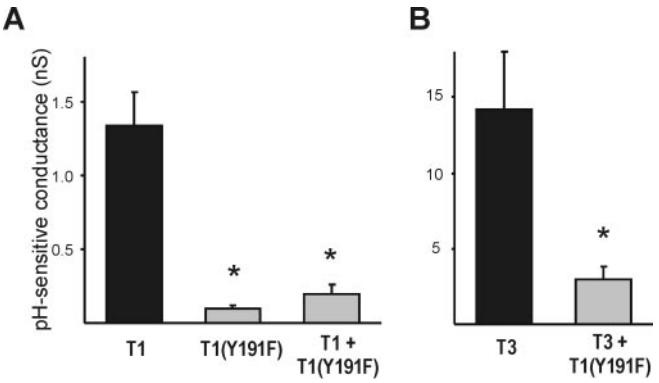

Figure 2. A TASK-1 construct bearing a point mutation in the second pore domain (Y191F) acts as a dominant negative of TASK-1 (T1) and TASK-3 (T3) channels. HEK 293 cells were transfected with the indicated constructs and recorded under whole-cell voltage clamp by using a ramp voltage protocol (−130 to 20 mV; 0.2 V/sec). Whole-cell conductance was calculated as the slope of the current evoked between −130 and − 60 mV, and the pH-sensitive conductance was determined as the difference in conductance at pH 8.4 and 5.9. *A*, Expression of TASK-1(Y191F) by itself generated no pH-sensitive conductance, and coexpression of TASK-1(Y191F) abolished the pH-sensitive conductance generated by wild-type TASK-1 (left; from 1.3 ± 0.2 to 0.1 ± 0.02 nS; $*p < 0.05$, ANOVA). A total of 6 μg of DNA was transfected in all cases, with TASK channel constructs transfected at 3 μg each and the balance provided by empty pcDNA3 vector. *B*, Importantly, TASK-1(Y191F) also eliminated pH-sensitive conductance from coexpressed TASK-3 channels (right; from 14.2 ± 3.8 to 3.0 ± 0.8 nS; $*p < 0.05$, *t* test). A total of 9 μg of DNA was transfected in each experiment, with GFP-TASK-3 at 2 μg and either TASK-1(Y191F) or pcDNA3 at 7 μg.

TASK-1(Y191F) channels generated essentially no pH-sensitive conductance in HEK 293 cells (0.1 ± 0.0 nS; $n = 14$; compared with 1.3 ± 0.2 nS; $n = 14$, for TASK-1 wild-type channels). When coexpressed with wild-type TASK-1, the mutant subunit reduced the pH-sensitive conductance to 0.2 ± 0.1 nS ($n = 12$). For coexpression of the TASK-1(Y191F) construct with TASK-3, we used an N-terminal GFP-tagged version of TASK-3. The currents generated by this construct were not different from those of the untagged channel (data not shown). We recorded GFP-TASK-3-transfected cells that displayed approximately the same level of surface membrane fluorescence under the two conditions [i.e., control vs cotransfection with TASK-1(Y191F)]. As illustrated in Figure 2*B*, and consistent with formation of heteromeric TASK channels, the mutant TASK-1(Y191F) construct strongly reduced the pH-sensitive conductance obtained from coexpressed TASK-3 channels (from 14.2 ± 3.8 nS; $n = 6$; to 3.0 ± 0.8 nS; $n = 6$). Thus, because cells coexpressing GFP-TASK-3 and TASK-1(Y191F) had much smaller pH-sensitive currents than control cells expressing GFP-TASK-3 alone, despite similar levels of membrane fluorescence, it appears that the effect of the dominant negative TASK-1(Y191F) subunit was to reduce current from channels that were targeted appropriately to the cell membrane.

We also generated the corresponding Y191F mutation in TASK-3; however, this construct did not function as a dominant negative. Instead, the TASK-3(Y191F) subunit produced functional open-rectifier K^+ channels but with a pH sensitivity enhanced relative to wild-type TASK-3 subunits (data not shown). The reason for these different effects of the same mutation in TASK-1 and TASK-3 subunits is unclear. Nonetheless, our data indicate that TASK-1(Y191F) functions as a dominant negative subunit and support the conclusion that TASK-1 and TASK-3 associate functionally when coexpressed in HEK 293 cells.

pH sensitivity of TASK-1/TASK-3 tandem heterodimeric channels

To characterize pharmacological properties of a homogenous population of heteromeric TASK channels, without contamination from homomeric channels, we recorded from recombinant tandem-linked TASK channels that joined the two subunits in a concatemeric arrangement, either as TASK-1/TASK-3 or as TASK-3/TASK-1. The tandem-linked TASK channels indeed form in *cis* as heterodimers (rather than as homodimers in *trans*) because we found that mutations that disrupt anesthetic- and receptor-mediated modulation of the channels are effective when placed in either subunit of the tandem (Talley and Bayliss, 2002).

We first compared the pH sensitivity of the tandem-linked heterodimeric TASK channels to that of homomeric TASK-1 or TASK-3 channels in HEK 293 cells. Voltage ramps were applied to individual cells, and whole-cell conductance was calculated from the slope of the *I–V* relationship between −130 and −60 mV as the pH of the bath solution was adjusted between pH 5.9 and 8.4. As depicted for representative cells (Fig. 3*A*), extreme bath acidification (from pH 7.3 to pH 5.9) caused a sharp decrease in whole-cell conductance in cells expressing any of the TASK channel constructs. The differences in pH sensitivity of the channels were most apparent with extreme alkalization (to pH 8.4); this was associated with a large increase in conductance relative to pH 7.3 in cells expressing either TASK-1 (69.6 ± 2.0%; $n = 6$) or the tandem heterodimers (48.4 ± 2.4%; $n = 11$) but only a modest increase in conductance in TASK-3-expressing cells (9.4 ± 1.7%; $n = 5$). The pH sensitivity curves for TASK homodimers and heterodimers were determined from logistic fits to averaged conductance data, normalized between pH 8.4 and 5.9, as shown in Figure 3*B* (left); data from TASK-1/TASK-3 and TASK-3/TASK-1 heterodimers were not different and were thus combined. These curves indicate that the pH sensitivity of the tandem constructs (pK ~7.3) is more like that of TASK-1 (pK ~7.5) than TASK-3 (pK ~6.8). Moreover, overlaying data from pH-sensitive currents in rat motoneurons (Talley et al., 2000) on the curves from cloned homodimeric and heterodimeric TASK channels indicates that, although the native pH-sensitive TASK-like conductance in motoneurons fits well to the TASK-1 curve, it corresponds even more closely to that of the TASK heterodimeric channels.

Differential isoflurane sensitivity of TASK channels

To establish a contribution of heterodimeric channels to TASK-like currents in motoneurons, we tested alternative pharmacological agents that might prove useful in distinguishing heterodimeric channels from their homomeric counterparts. We hoped that anandamide, a bioactive lipid that reportedly blocks currents from human TASK-1 but not human TASK-3 (Maingret et al., 2001), might provide a preferential modulation of TASK-1 homomeric but not TASK heteromeric channels. However, we found that homomeric rat TASK-1 and TASK-3 channels were not particularly sensitive to anandamide at 1 μM (TASK-1, 14.8 ± 5.0% inhibition; $n = 10$; TASK-3, 9.4 ± 5.9% inhibition; $n = 5$), and at a higher concentration (10 μM), inhibition was more robust, but effects on the two channels were too similar to be useful in distinguishing these channels in a native context (TASK-1, 62.1 ± 5.4% inhibition; $n = 10$; TASK-3, 46.5 ± 7.5% inhibition; $n = 4$). This was also the case for the stable analog methanandamide, which at 1 μM produced only a modest inhibition and at 10 μM was only slightly more effective at blocking TASK-1 than TASK-3 (TASK-1, 85.1 ± 2.7% inhibition; $n = 8$; TASK-3, 63.7 ± 6.8% inhibition; $n = 5$). Not surprisingly, given

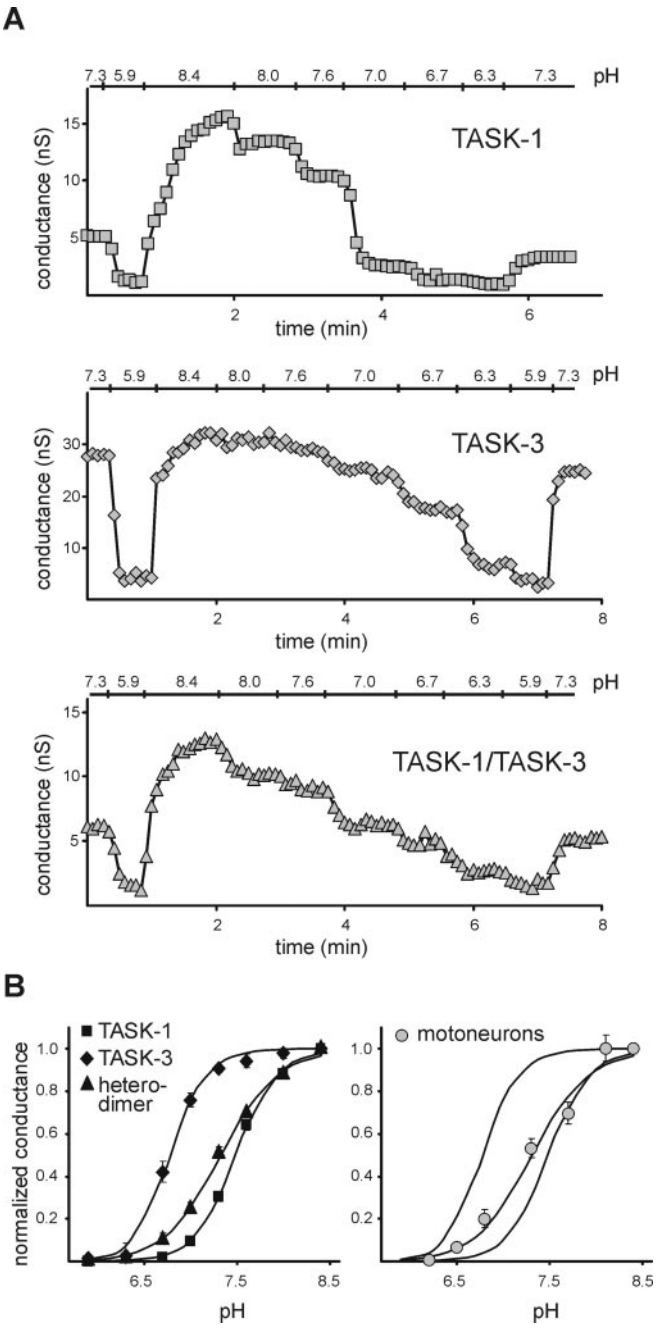

Figure 3. The pH sensitivity of TASK-like conductance in motoneurons resembles that of TASK-1/TASK-3 tandem heterodimeric channels. HEK 293 cells were transfected with cloned rat TASK-1, TASK-3, or tandem heterodimeric TASK-1/TASK-3 and TASK-3/TASK-1 constructs. *A*, Time series illustrating effects of changes in extracellular pH on whole-cell conductance (measured between −130 and −60 mV) in representative cells expressing TASK-1 (top), TASK-3 (middle), and TASK-1/TASK-3 (bottom). *B*, Left, pH sensitivity curves for TASK-1 (squares), TASK-3 (diamonds), and tandem heterodimers (pooled data from TASK-1/TASK-3 and TASK-3/TASK-1; triangles). Slope conductance at each bath pH was normalized to the total pH-sensitive conductance (pH 8.4–5.9) in individual cells and averaged; data points (mean ± SEM) were fitted with logistic equations (solid lines). The pK of the tandem heterodimer TASK channel constructs (pK ~7.3; $n = 11$) was closer to that of TASK-1 (pK ~7.5; $n = 6$) than to that of TASK-3 (pK ~6.8; $n = 5$). Right, The pH sensitivity of motoneuronal TASK-like current was determined in hypoglossal motoneurons recorded in brainstem slices from neonatal rats (Talley et al., 2000). The pH sensitivity of the native motoneuronal TASK-like currents (circles) overlays the fitted curve of the pH sensitivity of the tandem heterodimer TASK channels, with a pK of ~7.4 ($n = 9$).

these results with homomeric TASK-1 and TASK-3 channels, methanandamide was equally effective at inhibiting heteromeric TASK-1/TASK-3 channels (~15 and 55% inhibition at 1 and 10 μM, respectively). Therefore, although rodent TASK-1 may be slightly more sensitive than rodent TASK-3 to anandamide, the differences are not as pronounced as reported for the human channels (Maingret et al., 2001); moreover, it seems that the rodent TASK-1 is far less sensitive to anandamide than is its corresponding human ortholog (Maingret et al., 2001). Nevertheless, these data indicate that neither anandamide nor methanandamide provides a particularly sensitive tool either for distinguishing native currents attributable to homomeric TASK-1 and TASK-3 channels or for establishing a contribution of TASK channel heterodimers to native currents. It is worth pointing out that our results regarding the approximately equal sensitivity of rodent TASK-1 and TASK-3 to anandamide have been found by other researchers (D. Kim, personal communication).

We also tested agents that activate rather than inhibit TASK channels to determine whether those compounds modulate the subunits differentially. Volatile anesthetics, particularly halothane, activate TASK-1, TASK-3, and TASK-1/TASK-3 heterodimeric channels (Sirois et al., 1998, 2000; Patel et al., 1999; Meadows and Randall, 2001; Talley and Bayliss, 2002), although activation of TASK-1 was not as strong (Talley and Bayliss, 2002). Unexpectedly, we found that this differential anesthetic modulation of TASK channels was especially pronounced with the halogenated ether compound isoflurane. As shown for representative cells in Figure 4*A*, a high concentration of isoflurane (0.8 mM) increased pH-sensitive currents evoked by voltage ramps in individual cells expressing TASK-3 and TASK-1/TASK-3 but actually inhibited currents in TASK-1-expressing cells. These effects were fully reversible (Fig. 4*A*, insets). The effect of isoflurane was determined at different concentrations in individual cells and normalized to the maximal pH-sensitive conductance (Fig. 4*B*, left); at a concentration of 0.8 mM, isoflurane clearly discriminated between TASK-1 (-15 ± 2%, relative to total pH-sensitive conductance) and the other two channel constructs (TASK-3, $+138 \pm 25$%; TASK-1/TASK-3, $+106 \pm 7$%). These data differ from the initial report regarding the anesthetic sensitivity of human TASK-1, in which it was found that a high concentration of isoflurane (2 mM, applied at pH

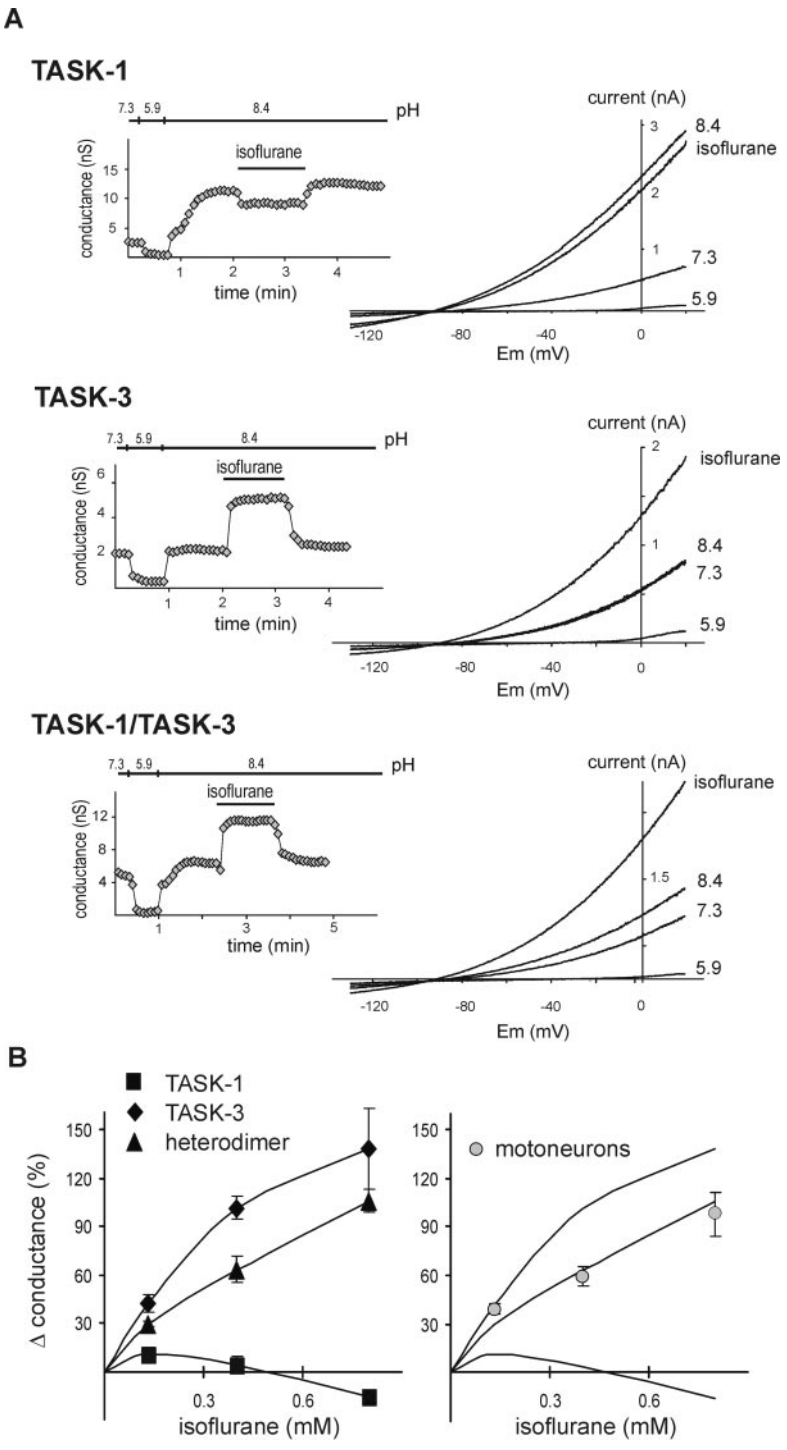

Figure 4. The isoflurane sensitivity of the TASK-like current in motoneurons resembles that of TASK-1/TASK-3 tandem heterodimeric channels. HEK 293 cells were transfected with rat TASK channel constructs and exposed to isoflurane at concentrations of 0.13, 0.4, and 0.8 mM. *A*, Whole-cell current was measured from cells expressing TASK-1 (top), TASK-3 (middle), and TASK-1/TASK-3 (bottom) during depolarizing ramps (−130 to 20 mV; 0.2 V/sec) and plotted against membrane potential (Em) under control conditions, pH 7.3, and during bath acidification, pH 5.9, bath alkalization, pH 8.4, and exposure to isoflurane in an alkalized bath (0.8 mM isoflurane). Insets, Time series illustrating effects on whole-cell conductance of changing bath pH and of 0.8 mM isoflurane for each cell represented in the corresponding *I–V* plots. *B*, Left, Dose–response curves illustrating effects of isoflurane on rat TASK-1 (squares), TASK-3 (diamonds), or the tandem heterodimeric TASK-1/TASK-3 construct (triangles). Slope conductance at each isoflurane concentration was normalized to the total pH-sensitive conductance in individual cells and averaged; data points (mean ± SEM) were fitted with logistic equations (solid lines). Differences in effects of isoflurane on the TASK constructs were highly significant ($F_{(2,37)} = 90$; $p < 0.0001$, ANOVA); at the highest concentration, isoflurane increased TASK-3 and TASK-1/TASK-3 channel currents (both $p < 0.05$; $n = 5$; $n = 8$), whereas it inhibited TASK-1 current ($p < 0.05$; $n = 5$). Right, Effects of isoflurane on the native TASK-like conductance were determined in rat hypoglossal motoneurons, normalized to total pH-sensitive conductance, and averaged (±SEM; circles); the isoflurane sensitivity of the motoneuronal conductance overlays most closely that of the TASK channel heterodimer.

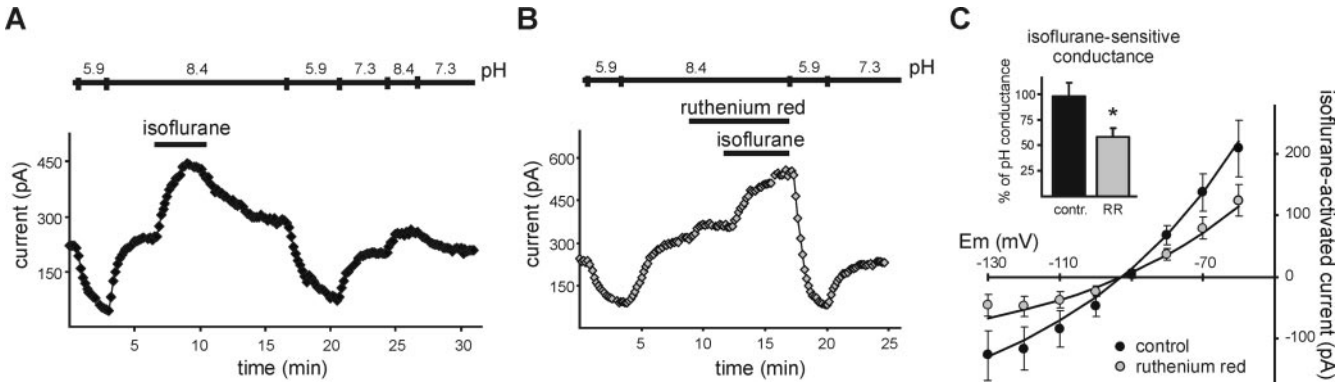

Figure 5. The pH sensitivity of native motoneuronal currents, together with the isoflurane sensitivity of ruthenium red-resistant currents, indicates a contribution from TASK channel heterodimers. Whole-cell voltage-clamp recordings were obtained at −60 mV from hypoglossal motoneurons in brainstem slices from rat pups to determine effects of bath pH and a discriminating concentration of isoflurane (0.8 mM) on membrane current. *A*, Relative to control conditions, pH 7.3, bath acidification to pH 5.9 decreased motoneuronal outward current, whereas bath alkalization to pH 8.4 increased outward current, with the difference representing the total pH-sensitive current. Isoflurane caused a robust increase in outward current typical for effects on TASK-3 or TASK channel heterodimers. *B*, After defining the pH-sensitive current, ruthenium red (10 μM) was applied to block TASK-3 channels; application of ruthenium red invariably increased outward current, suggesting effects on multiple conductances. In the continuous presence of ruthenium red, 0.8 mM isoflurane caused a large increase in membrane current. *C*, The averaged isoflurane-sensitive current (±SEM) in the absence (control, filled circles; $n = 5$) and presence (shaded circles; $n = 8$) of ruthenium red was plotted against membrane potential and was well fitted by using the Goldman–Hodgkin–Katz current equation indicating open-rectifier K^+ conductance. Inset, The isoflurane-sensitive conductance was normalized to the total pH-sensitive conductance in each cell and averaged (±SEM) for control conditions and in the presence of 10 μM ruthenium red. *$p < 0.05$, *t* test.

7.4) modestly activated the channel (by ~20%) (Patel et al., 1999). The reason for this discrepancy is not clear, but it may reflect differences between human and rodent orthologs of the channel because we also found that isoflurane inhibited rodent TASK-1 currents when tested at pH 7.4 (approximately −7%; $n = 5$), even at concentrations up to ~1.7 mM (data not shown). In any case, when data describing effects of isoflurane on rat motoneurons were overlaid on the fitted curves of isoflurane sensitivity from cloned rat TASK channels (Fig. 4*B*, right), it was apparent that values from motoneurons were most consistent with those from the heterodimeric TASK channel construct.

The pH and isoflurane sensitivity of hypoglossal motoneurons suggests a contribution from TASK heteromeric channels

As noted above, our previous findings regarding the pH and isoflurane sensitivity of native TASK-like currents in motoneurons suggest an underlying contribution from TASK heterodimeric channels (Figs. 3*B*, 4*B*). Our previous data on the pH sensitivity of motoneurons (Talley et al., 2000) and the current results on isoflurane activation were obtained from two different groups of cells. Because these different populations might have preferentially expressed TASK-1 or TASK-3, we used a three-point titration to assess pH sensitivity in individual motoneurons also tested with isoflurane (Fig. 5). As shown in Figure 5*A*, hypoglossal motoneurons that responded strongly to isoflurane with increased outward current and conductance did so also when challenged with bath alkalization (from pH 7.3 to pH 8.4). In fact, changes in bath pH from 5.9 to 7.3 and from 7.3 to 8.4 caused approximately equal incremental increases in conductance. The current activation by both isoflurane and bath alkalization is particularly notable with respect to a contribution by heterodimeric TASK channels because, in isolation, neither homomeric TASK-1 or TASK-3 channels can account for both these effects. Overall, we found that isoflurane induced a 97.6 ± 13.5% increase in conductance (relative to total pH-sensitive conductance), and, in the same cells, bath alkalization from pH 7.3 to 8.4 accounted for 30.8 ± 6.5% of pH-sensitive conductance ($n = 5$). Therefore, our results from individual cells are consistent with earlier data from separate groups of motoneurons and indicate that these properties of native currents, both pH and isoflurane sensitivity, can be best represented by TASK heterodimeric channels.

A ruthenium red-resistant and isoflurane-sensitive open-rectifier K^+ current indicates a prominent contribution of TASK heteromeric channels in hypoglossal motoneurons

One could argue that there is no need to invoke a contribution of native TASK-1/TASK-3 channels if the pH sensitivity of motoneuronal TASK-like currents is contributed disproportionately by TASK-1 homomeric channels, with a latent fraction of TASK-3 homomeric channels revealed more fully in the presence of isoflurane. To rule this out and to provide more certain evidence for involvement of TASK heterodimeric channels in the motoneuronal currents, we tested the effect of isoflurane after blocking TASK-3 homodimeric channels. Among TASK channels, ruthenium red potently and selectively blocks TASK-3 homodimers, with essentially no effect on TASK-1 homodimers or TASK heterodimers (~85% inhibition of TASK-3 channels) (Czirjak and Enyedi, 2002a, 2003; Kang et al., 2003). As shown for a representative motoneuron in Figure 5*B*, isoflurane induced a strong increase in current, even in the presence of 10 μM ruthenium red. Note that ruthenium red caused a slight increase in outward current rather than the decrease expected from inhibition of TASK-3 channels. It is well known that this compound is active at various sites [e.g., ryanodine receptors (Hohenegger et al., 2002) and TRPV channels (Guler et al., 2002)], so it is perhaps not surprising that it has multiple effects in these neurons. Nevertheless, exactly as expected for open-rectifier K^+ channels, the *I–V* relationship of the isoflurane-sensitive current was well fitted by the Goldman–Hodgkin–Katz equation with a reversal potential near E_K (Fig. 5*C*) either in the presence (shaded circles) or the absence (filled circles) of ruthenium red. The total pH-sensitive current (i.e., before ruthenium red application) was essentially identical in these two groups of cells (control, 301.0 ± 96.4 pA; $n = 5$; ruthenium red, 307.8 ± 40.1 pA; $n = 7$), but the magnitude of the isoflurane current was reduced in cells treated with ruthenium red, consistent with inhibition of TASK-3 homomeric channels in these cells. On average, isoflurane induced a 58.4 ±

8.7% increase in conductance ($n = 7$; relative to total pH-sensitive conductance) when TASK-3 channels were blocked by ruthenium red, an effect significantly smaller than that seen in the absence of ruthenium red (97%; see above). This suggests that TASK-3 homomeric channels provide a substantial contribution to the isoflurane-sensitive TASK-like current in motoneurons. However, given that TASK-1 homomeric channels are not enhanced by isoflurane (Fig. 4), the considerable residual motoneuronal TASK-like current induced by isoflurane in the presence of ruthenium red must include a contribution from TASK-1/TASK-3 heteromeric channels.

The fact that ruthenium red appeared to have multiple effects on motoneurons, in addition to blocking TASK-3 homomeric channels, precluded a precise quantitative determination of the homomeric TASK-3 contribution to the motoneuronal TASK-like current. However, an estimate can be obtained if one considers effects of 0.8 mM isoflurane on motoneuronal currents under standard conditions (approximately +100%) and after blocking TASK-3 homodimeric channels with ruthenium red (approximately +60%), together with effects of isoflurane on recombinant TASK-3 homomeric channels (+140%, all relative to total pH-sensitive conductance). Thus, the TASK-3 contribution to the pH-sensitive conductance is given by $(100 - 60)/140 * 100 = 29\%$, which when corrected for the incomplete block by ruthenium red is ~34% (29%/0.85). Likewise, the ruthenium red-resistant current modulated by isoflurane (+60%) can be used to deduce the relative contributions of homomeric TASK-1 and heteromeric TASK-1/TASK-3 channels to the native motoneuronal pH-sensitive current, given the effects of 0.8 mM isoflurane determined for recombinant channels (TASK-1, approximately −15%; TASK-1/TASK-3, approximately +105%) (Fig. 4*B*) and again assuming ~85% block of homomeric motoneuronal TASK-3 channels by 10 μM ruthenium red. This analysis suggests a small contribution from TASK-1 homomeric channels (~14%) and a much larger contribution from heteromeric TASK channels (~52%) [i.e., $(14\% * -0.15) + (52\% * 1.05) + (34\% * 1.4 * 0.15) = 60\%$]. Thus, these calculations based on data from the isoflurane and ruthenium red experiments suggest a predominant contribution from heteromeric TASK-1/TASK-3 channels to native motoneuronal currents.

As a further validation of this estimate, we applied our calculated fractional contributions as a weighting factor to the pH and isoflurane sensitivity curves that were determined from cloned homomeric and heteromeric channels and fit the sum of those curves with logistic equations. This analysis, shown in Figure 6, provides the pH and isoflurane sensitivity that would be expected given the relative contributions of TASK channels that we estimated for motoneurons (TASK-1, 14%; TASK-1/TASK-3, 52%; TASK-3, 34%). These predicted concentration–response curves also fit the overlaid isoflurane and pH sensitivity of TASK-like currents from motoneurons extremely well.

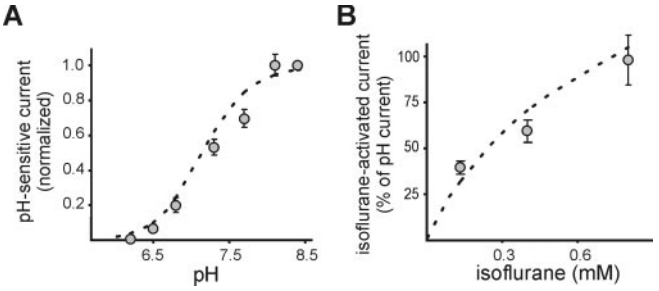

Figure 6. The measured pH and isoflurane sensitivity of motoneurons are well described by curves derived from estimates of the relative contributions of TASK homodimers and heterodimers to native currents. Data from experiments with combined application of ruthenium red and isoflurane were used to estimate the fractional contribution of TASK-1 homodimers, TASK-3 homodimers, and TASK-1/TASK-3 heterodimers to the whole-cell pH-sensitive current in motoneurons (TASK-1, ~14%; TASK-3, ~34%; TASK heterodimers, ~52%; see Results). These fractional contributions were applied as weighting factors to the pH and isoflurane sensitivity curves determined for cloned TASK channels, which were then summed and fitted to determine a predicted pH (*A*) and isoflurane (*B*) sensitivity of motoneuronal TASK-like currents. In both cases, these predicted sensitivity curves (dashed lines) closely matched data obtained from motoneurons (circles).

Discussion

The ability of closely related K^+ channel subunits to associate into functional heteromeric channels is now well established within the voltage-gated and inwardly rectifying K^+ channel families (Wei et al., 1990; Krapivinsky et al., 1995; Wang et al., 1998). In contrast, the existence of native heteromeric channels comprising subunits of the more recently described two-pore-domain KCNK family of background K^+ channels has been less certain. Our experiments in a mammalian heterologous system expressing cloned TASK channel subunits provide biochemical and electrophysiological support for the contention that these particular KCNK subunits are capable of functional coassociation. The pH sensitivity of recombinant TASK heterodimeric channels was intermediate between TASK-1 and TASK-3 homomeric channels and remarkably similar to the pH sensitivity of native motoneuronal TASK-like currents. Moreover, we discovered a marked selectivity in TASK channel sensitivity to the inhalational anesthetic isoflurane; TASK-1 homodimeric channels were inhibited by isoflurane, whereas both TASK-3 homodimeric and TASK heterodimeric channels were strongly activated. We used this characteristic pH and isoflurane sensitivity, along with a previously described TASK subunit-selective sensitivity to ruthenium red (Czirjak and Enyedi, 2002a, 2003; Kang et al., 2003), to establish a contribution of TASK heterodimeric channels to native motoneuronal TASK-like currents. Specifically, we found an isoflurane-activated open-rectifier K^+ current in motoneurons that was substantial even after blocking TASK-3 homomeric channels with ruthenium red; this residual isoflurane-resistant TASK-like current could only be attributed to TASK heterodimeric channels. Therefore, in motoneurons that strongly express TASK-1 and TASK-3 subunits (Karschin et al., 2001; Talley et al., 2001), the formation of TASK heterodimeric channels provides a major component of background K^+ current with unique modulatory properties.

Heterologously expressed TASK-1 and TASK-3 can form heterodimeric channels

The data we present indicate that TASK channel subunits co-expressed in mammalian cells can coassociate and form functional heterodimeric TASK channels. The ability of TASK subunits to form heterodimeric channels has been tested previously in other expression systems and with other approaches, but the results have not been uniformly positive (Karschin et al., 2001; Czirjak and Enyedi, 2002a; Kang et al., 2003; Lauritzen et al., 2003; Pei et al., 2003). It is clear that a tandem-linked construct, in which the two TASK subunits are concatenated into a single polypeptide, supports formation of heterodimeric channels and allows their functional and pharmacological characterization (Czirjak and Enyedi, 2002a; Talley and Bayliss, 2002; Kang et al., 2003). The kinetic and voltage-dependent properties of whole-cell currents from these heteromeric TASK channels are essentially identical to those of homomeric channels, making it impos-

sible to identify heterodimeric channels by relying only on those basic properties. Likewise, the pH sensitivity of expressed currents cannot be used as a sole diagnostic criteria for heterodimer formation because mixed populations of TASK-1 and TASK-3 homomeric channels could lead to an intermediate pH sensitivity like that of TASK heterodimeric channels. However, by taking advantage of the distinct combined pH and ruthenium red sensitivity of the heterodimers, it was possible to identify an expressed current with kinetic and pharmacological properties consistent with heterodimeric TASK channels after coinjection of TASK-1 and TASK-3 mRNA in *Xenopus laevis* oocyte expression (Czirjak and Enyedi, 2002a).

A dominant negative approach has been used to establish coassociation of different subunits in other families of K^+ channels. In the case of TASK channels, this approach produced conflicting reports, even when using the same dominant negative construct (Karschin et al., 2001; Lauritzen et al., 2003; Pei et al., 2003). Thus, a TASK-3(G95E) construct reportedly did not disrupt currents from wild-type TASK-1 subunits in *Xenopus* oocytes (Karschin et al., 2001; Pei et al., 2003), whereas in a separate study, that same TASK-3(G95E) channel blocked wild-type TASK-1 currents, and, in addition, a TASK-1(G95E) construct abrogated currents from oocytes coinjected with wild-type TASK-3 subunits (Lauritzen et al., 2003). We identified a new dominant negative TASK-1 channel construct analogous to that used to abolish conductance in voltage-gated channels and showed that this TASK-1(Y191F) subunit nearly completely blocked currents from cotransfected wild-type TASK-3 channels. Thus, in agreement with the latter study using TASK(G95E) mutant subunits, our data support the interpretation that TASK-1 and TASK-3 can indeed form heterodimeric channels. Moreover, we have buttressed this conclusion by also showing that TASK-1 and TASK-3 can be coimmunoprecipitated from membranes of cells cotransfected with the channel subunits.

Native TASK heterodimeric channels are prominently expressed in rat hypoglossal motoneurons

As mentioned, the identification of native TASK heterodimeric channels has been hindered by the fact that the heterodimeric channel shares key functional properties with both TASK-1 and TASK-3 homomeric channels. To circumvent this, we took advantage of a pharmacological profile that is unique among TASK subunits to the heterodimeric channel, sensitivity to isoflurane and resistance to ruthenium red, to define a contribution of TASK heterodimers to the native background K^+ current in motoneurons. In cerebellar granule neurons, an approach based on single-channel analysis was used to identify native TASK heterodimeric channels among a mixed population of TASK homodimeric and heterodimeric channels (Kang et al., 2003). In that study, it was noted that TASK-1/TASK-3 heterodimeric channels have a unitary conductance (~38 pS under the defined conditions) that is twice that of TASK-1 but virtually indistinguishable from that of TASK-3; because among these channels only TASK-3 is sensitive to ruthenium red, the demonstration of native TASK-like 38 pS channels that were resistant to ruthenium red among a mixed population of TASK-like channels provided very strong evidence that the recorded channels represented TASK heterodimers (Kang et al., 2003).

We were able to estimate indirectly the relative contributions of different populations of homodimeric and heterodimeric TASK channels to the native motoneuronal current, an estimate that suggested that ~52% of the motoneuronal TASK-like current could be attributed to TASK-1/TASK-3 channels. This calculation appears to be reasonable because the combined pH and isoflurane sensitivity curves of the cloned channels, each weighted according to the estimate, provided a remarkably good representation of the pH- and isoflurane-sensitive TASK-like currents in motoneurons (see Fig. 6). In other cells coexpressing both TASK-1 and TASK-3, a substantial contribution of TASK heterodimers to native currents has not been clearly established. For example, in adrenal glomerulosa cells and cerebellar granule neurons, the whole-cell TASK-like current is nearly completely blocked by ruthenium red (Czirjak and Enyedi, 2002b; Lauritzen et al., 2003), indicating that TASK-3 homodimeric channels predominate; it was not determined whether the smaller residual, ruthenium red-resistant current in these cells was attributable mostly to TASK-1 homodimeric channels or if TASK-1/TASK-3 heterodimeric channels also contributed. It is worth pointing out, however, that estimates based on the density of single TASK heterodimeric channels in cerebellar granule neurons suggested that they make a greater contribution to whole-cell currents in those neurons (approximately equal to that of TASK-3 homomeric channels) (Kang et al., 2003).

Physiological and clinical consequences of TASK-1/TASK-3 heterodimers

Our findings indicate that TASK heterodimeric channels provide a major component of the pH-sensitive open-rectifier TASK-like current in motoneurons. This is consistent with previous work because the pH sensitivity of the motoneuronal currents (Talley et al., 2000) was very similar to that predicted by the admixture of TASK homodimeric and heterodimeric channels estimated from this work (see Fig. 6*A*). In motoneurons and in other neuronal cell groups in which both channels are expressed (Karschin et al., 2001; Talley et al., 2001; Vega-Saenz de Miera et al., 2001), the potential to assemble channels in homomeric or heteromeric configurations provides a mechanism for increasing diversity of leak K^+ channel properties. For example, changes in the relative expression of TASK-1 and TASK-3, as happens in cerebellar granule neurons through development (Han et al., 2002; Lauritzen et al., 2003), could serve to favor formation of different combinations of homomeric or heteromeric TASK channels and thereby regulate the pH range over which cells respond.

It now seems clear that inhalation anesthetics can activate native TASK channels in a clinically relevant concentration range and thereby inhibit neuronal excitability (Sirois et al., 1998, 2000; Patel et al., 1999; Meadows and Randall, 2001; Talley and Bayliss, 2002). We have suggested that anesthetic activation of TASK channels in motoneurons and in aminergic brainstem neurons could contribute to their immobilizing and soporific effects (Sirois et al., 1998, 2000, 2002; Bayliss et al., 2001; Talley and Bayliss, 2002). Here, we made the unexpected observation that TASK-3 homomeric and TASK-1/TASK-3 heterodimeric channels are sensitive to isoflurane, whereas TASK-1 homomeric channels were relatively unaffected. It remains to be determined which, if any, anesthetic end points result from isoflurane actions on TASK channels, but these data indicate that those effects require a contribution from TASK-3 subunits, either in a homomeric channel or combined with TASK-1 in a heteromeric channel.

References

Bayliss DA, Talley EM, Sirois JE, Lei Q (2001) TASK-1 is a highly modulated pH-sensitive "leak" K^+ channel expressed in brainstem respiratory neurons. Respir Physiol 129:159–174.

Bayliss DA, Sirois JE, Talley EM (2003) The TASK family: two-pore domain background K^+ channels. Mol Interv 3:205–219.

Chapman CG, Meadows HJ, Godden RJ, Campbell DA, Duckworth M, Kelsell RE, Murdock PR, Randall AD, Rennie GI, Gloger IS (2000) Cloning, localisation and functional expression of a novel human, cerebellum specific, two pore domain potassium channel. Brain Res Mol Brain Res 82:74–83.

Chemin J, Girard C, Duprat F, Lesage F, Romey G, Lazdunski M (2003) Mechanisms underlying excitatory effects of group I metabotropic glutamate receptors via inhibition of 2P domain K^+ channels. EMBO J 22:5403–5411.

Czirjak G, Enyedi P (2002a) Formation of functional heterodimers between the TASK-1 and TASK-3 two-pore domain potassium channel subunits. J Biol Chem 277:5426–5432.

Czirjak G, Enyedi P (2002b) TASK-3 dominates the background potassium conductance in rat adrenal glomerulosa cells. Mol Endocrinol 16:621–629.

Czirjak G, Enyedi P (2003) Ruthenium red inhibits TASK-3 potassium channel by interconnecting glutamate 70 of the two subunits. Mol Pharmacol 63:646–652.

Czirjak G, Fischer T, Spat A, Lesage F, Enyedi P (2000) TASK (TWIK-related acid-sensitive K^+ channel) is expressed in glomerulosa cells of rat adrenal cortex and inhibited by angiotensin II. Mol Endocrinol 14:863–874.

Duprat F, Lesage F, Fink M, Reyes R, Heurteaux C, Lazdunski M (1997) TASK, a human background K^+ channel to sense external pH variations near physiological pH. EMBO J 16:5464–5471.

Goldstein SA, Bockenhauer D, O'Kelly I, Zilberberg N (2001) Potassium leak channels and the KCNK family of two-P-domain subunits. Nat Rev Neurosci 2:175–184.

Guler AD, Lee H, Iida T, Shimizu I, Tominaga M, Caterina M (2002) Heat-evoked activation of the ion channel, TRPV4. J Neurosci 22:6408–6414.

Han J, Truell J, Gnatenco C, Kim D (2002) Characterization of four types of background potassium channels in rat cerebellar granule neurons. J Physiol (Lond) 542:431–444.

Hohenegger M, Suko J, Gscheidlinger R, Drobny H, Zidar A (2002) Nicotinic acid-adenine dinucleotide phosphate activates the skeletal muscle ryanodine receptor. Biochem J 367:423–431.

Kang D, Han J, Talley EM, Bayliss DA, Kim D (2003) Functional expression of TASK-1/TASK-3 heteromers in cerebellar granule cells. J Physiol (Lond) 554:64–77.

Karschin C, Wischmeyer E, Preisig-Muller R, Rajan S, Derst C, Grzeschik KH, Daut J, Karschin A (2001) Expression pattern in brain of TASK-1, TASK-3, and a tandem pore domain K^+ channel subunit, TASK-5, associated with the central auditory nervous system. Mol Cell Neurosci 18:632–648.

Kim D, Fujita A, Horio Y, Kurachi Y (1998) Cloning and functional expression of a novel cardiac two-pore background K^+ channel (cTBAK-1). Circ Res 82:513–518.

Kim GD, Carr IC, Anderson LA, Zabavnik J, Eidne KA, Milligan G (1994) The long isoform of the rat thyrotropin-releasing hormone receptor down-regulates G_q proteins. J Biol Chem 269:19933–19940.

Kim Y, Bang H, Kim D (2000) TASK-3, a new member of the tandem pore K^+ channel family. J Biol Chem 275:9340–9347.

Krapivinsky G, Gordon EA, Wickman K, Velimirovic B, Krapivinsky L, Clapham DE (1995) The G-protein-gated atrial K^+ channel IK_{ACh} is a heteromultimer of two inwardly rectifying K^+-channel proteins. Nature 374:135–141.

Lauritzen I, Zanzouri M, Honore E, Duprat F, Ehrengruber MU, Lazdunski M, Patel AJ (2003) K^+-dependent cerebellar granule neuron apoptosis: role of TASK leak K^+ channels. J Biol Chem 278:32068–32076.

Leonoudakis D, Gray AT, Winegar BD, Kindler CH, Harada M, Taylor DM, Chavez RA, Forsayeth JR, Yost CS (1998) An open rectifier potassium channel with two pore domains in tandem cloned from rat cerebellum. J Neurosci 18:868–877.

Lesage F (2003) Pharmacology of neuronal background potassium channels. Neuropharmacology 44:1–7.

Lesage F, Lazdunski M (2000) Molecular and functional properties of two-pore-domain potassium channels. Am J Physiol Renal Physiol 279:F793–F801.

Maingret F, Patel AJ, Lazdunski M, Honore E (2001) The endocannabinoid anandamide is a direct and selective blocker of the background K^+ channel TASK-1. EMBO J 20:47–54.

Malin SA, Nerbonne JM (2000) Elimination of the fast transient in superior cervical ganglion neurons with expression of KV4.2W362F: molecular dissection of I_A. J Neurosci 20:5191–5199.

Mattingly RR, Sorisky A, Brann MR, Macara IG (1994) Muscarinic receptors transform NIH 3T3 cells through a Ras-dependent signalling pathway inhibited by the Ras-GTPase-activating protein SH3 domain. Mol Cell Biol 14:7943–7952.

Meadows HJ, Randall AD (2001) Functional characterisation of human TASK-3, an acid-sensitive two-pore domain potassium channel. Neuropharmacology 40:551–559.

Nakamura RL, Anderson JA, Gaber RF (1997) Determination of key structural requirements of a K^+ channel pore. J Biol Chem 272:1011–1018.

Patel AJ, Honore E (2001) Properties and modulation of mammalian 2P domain K^+ channels. Trends Neurosci 24:339–346.

Patel AJ, Honore E, Lesage F, Fink M, Romey G, Lazdunski M (1999) Inhalational anesthetics activate two-pore-domain background K^+ channels. Nat Neurosci 2:422–426.

Pei L, Wiser O, Slavin A, Mu D, Powers S, Jan LY, Hoey T (2003) Oncogenic potential of TASK3 (Kcnk9) depends on K^+ channel function. Proc Natl Acad Sci USA 100:7803–7807.

Perozo E, MacKinnon R, Bezanilla F, Stefani E (1993) Gating currents from a nonconducting mutant reveal open-closed conformations in Shaker K^+ channels. Neuron 11:353–358.

Rajan S, Wischmeyer E, Xin LG, Preisig-Muller R, Daut J, Karschin A, Derst C (2000) TASK-3, a novel tandem pore domain acid-sensitive K^+ channel: an extracellular histidine as pH sensor. J Biol Chem 275:16650–16657.

Rajan S, Wischmeyer E, Karschin C, Preisig-Muller R, Grzeschik KH, Daut J, Karschin A, Derst C (2001) THIK-1 and THIK-2, a novel subfamily of tandem pore domain K^+ channels. J Biol Chem 276:7302–7311.

Schroeder BC, Hechenberger M, Weinreich F, Kubisch C, Jentsch TJ (2000) KCNQ5, a novel potassium channel broadly expressed in brain, mediates M-type currents. J Biol Chem 275:24089–24095.

Sirois JE, Pancrazio JJ, Lynch III C, Bayliss DA (1998) Multiple ionic mechanisms mediate inhibition of rat motoneurones by inhalation anaesthetics. J Physiol (Lond) 512:851–862.

Sirois JE, Lei Q, Talley EM, Lynch III C, Bayliss DA (2000) The TASK-1 two-pore domain K^+ channel is a molecular substrate for neuronal effects of inhalation anesthetics. J Neurosci 20:6347–6354.

Sirois JE, Lynch III C, Bayliss DA (2002) Convergent and reciprocal modulation of a leak K^+ current and I_h by an inhalational anaesthetic and neurotransmitters in rat brainstem motoneurones. J Physiol (Lond) 541:717–729.

Talley EM, Bayliss DA (2002) Modulation of TASK-1 (Kcnk3) and TASK-3 (Kcnk9) potassium channels: volatile anesthetics and neurotransmitters share a molecular site of action. J Biol Chem 277:17733–17742.

Talley EM, Lei Q, Sirois JE, Bayliss DA (2000) TASK-1, a two-pore domain K^+ channel, is modulated by multiple neurotransmitters in motoneurons. Neuron 25:399–410.

Talley EM, Solorzano G, Lei Q, Kim D, Bayliss DA (2001) CNS distribution of members of the two-pore-domain (KCNK) potassium channel family. J Neurosci 21:7491–7505.

Talley EM, Sirois JE, Lei Q, Bayliss DA (2003) Two-pore-Domain (KCNK) potassium channels: dynamic roles in neuronal function. Neuroscientist 9:46–56.

Vega-Saenz de Miera E, Lau DH, Zhadina M, Pountney D, Coetzee WA, Rudy B (2001) KT3.2 and KT3.3, two novel human two-pore K^+ channels closely related to TASK-1. J Neurophysiol 86:130–142.

Wang HS, Pan Z, Shi W, Brown BS, Wymore RS, Cohen IS, Dixon JE, McKinnon D (1998) KCNQ2 and KCNQ3 potassium channel subunits: molecular correlates of the M-channel. Science 282:1890–1893.

Washburn CP, Sirois JE, Talley EM, Guyenet PG, Bayliss DA (2002) Serotonergic raphe neurons express TASK channel transcripts and a TASK-like pH- and halothane-sensitive K^+ conductance. J Neurosci 22:1256–1265.

Wei A, Covarrubias M, Butler A, Baker K, Pak M, Salkoff L (1990) K^+ current diversity is produced by an extended gene family conserved in *Drosophila* and mouse. Science 248:599–603.